Characterisation of bare and tannase-loaded calcium alginate beads by microscopic, thermogravimetric, FTIR and XRD analyses

Claudio Larosa[a]

Marco Salerno[b]

Juliana Silva de Lima[c]

Remo Merijs Meri[d]

Milena Fernandes da Silva[e]

Luiz Bezerra de Carvalho[c]

Attilio Converti[a, *]

converti@unige.it

[a]Department of Civil, Chemical and Environmental Engineering, University of Genoa, Pole of Chemical Engineering, via Opera Pia 15, 16145 Genoa, Italy

[b]Materials Characterization Facility, Istituto Italiano di Tecnologia, via Morego 30, 16163 Genoa, Italy

[c]Laboratory of Immunopathology Keizo Asami (LIKA), Department of Biochemistry, Federal University of Pernambuco, Av. Prof. Moraes Rego, Recife, PE 50670-901, Brazil

[d]Riga Technical University, Faculty of Materials Science and Applied Chemistry, Institute of Polymer Materials, 3 Paula Valdena Street, Lv 1048 Riga, Latvia

[e]Bioscience Center, Federal University of Pernambuco, Av. Prof. Moraes Rego 1235, Cidade Universitária, 50670-420 Recife, PE, Brazil

*Corresponding author.

Abstract

Incorporating enzymes into calcium alginate beads is an effective method to immobilize them and to preserve, at the same time, their catalytic activity. Sodium alginate was mixed with *Aspergillus ficuum* tannase in aqueous solution, and tannase-loaded calcium alginate beads were prepared using a simple droplet-based microfluidic system. Extensive experimental analysis was carried out to characterise the samples. Microscopic imaging revealed morphological differences between the surfaces of bare alginate matrix and tannase-loaded alginate beads. Thermal analysis allowed assessing the hydration contents of alginate and revealed the presence of tannase entrapped in the loaded beads, which was also confirmed by vibrational spectroscopy. X-ray diffraction allowed us to conclude that alginate of tannase-loaded beads is not crystalline, which would make them suitable as carriers for possible controlled release. Moreover, they could be used in food applications to improve tea quality or clarify juices.

Keywords: Calcium alginate beads; Tannase; Fourier-transform infrared spectroscopy; Differential scanning calorimetry; X-ray diffraction

1. Introduction

Alginic acid is a natural anionic heteropolysaccharide present in the cell-wall of brown seaweeds, which is insoluble in its acidic form [1]. Its carboxylic groups are responsible, mainly in their ionised form, for its metal adsorption capacity. Alginates are known for decades thanks to their natural abundance and biological properties, which make them suitable in many applications in the medical, food, cosmetic, pharmaceutical and surgical sectors [2–4]. In food and pharmaceutical industries, alginate is widely used as gelling agent when crosslinked with divalent ions like calcium and ferrous cations [5]. The alginate gels are also suitable for biomedical applications and as material for cell immobilization, due to its high biocompatibility, low cost, safety and mild gelation process [6]. In the medical field alginates enhance the removal of viscous mucus, which helps in making the cough more productive and less frequent, and are also used to reduce chest congestion caused by common cold, infections or allergies [7]. Alginic acid forms salts with many bivalent cations, particularly Ca^{2+}, Sr^{2+} ((Sr^{2+})) and Ba^{2+}, which are insoluble in water

[8–10]. Among other alginate salts, sodium alginate has found pharmaceutical use in drug carriers thanks to its physical properties [11,12], allowing for gel preparation that enables the ~~delivery~~release of entrapped biomolecules such as drugs, peptides, and proteins [13]. Na-alginate is a linear polymer composed of β-D-mannuronic (M) and α-L-guluronic (G) acids, which can be inter-connected by substituting Na^+ by Ca^{2+} in consecutive blocks of G-unities (gelation). This interaction permits the formation of an egg-box like structure, which is effective to entrap cells and macromolecules. Sodium alginate is also able to stabilise dispersed compounds and can prevent the crystal growth in protein formulations, which would change their homogeneity and appearance. The thermal behaviour of alginate composites is important in the formulation of gel materials for the above-mentioned application, also in connection with the gel water content; for this reason, their inactivation and decomposition performance versus temperature have to be assessed.

The formation and the mechanical and structural properties of alginate beads depend on different parameters such as the alginate composition and concentration ratio that finally determine the gel viscosity, the presence of impurities in the polysaccharide, the nature and concentration of the gelling ion, and the gelation conditions [14], among others. Therefore, obtaining reproducible performance is a challenge, and the method is far from effective standardization.

Tannin acyl hydrolases (EC, 3.1.1.20), commonly referred to as tannases, are inducible enzymes produced by fungi, yeast and bacteria [11] that cleave ester and depside linkages in hydrolysable tannins [11,15] and synthesize gallic acid esters [16] by catalysing esterification/trans esterification reactions in organic media [17]. Tannases are used in various industrial sectors such as food, beverage and pharmaceutical industry as well as in feed for breeding animals, with special concern to produce instant tea, corn liquor, beer and fruit juice [18,19]. Research efforts focused on tea quality deal with a) hydrolysis of catechins to increase antioxidant activity and prevent, at the same time, cream formation [20], and b) improvement of col~~o~~our appearance, digestibility and overall sensory acceptance [21,22]. However, tannases show insufficient stability resulting in low catalytic performance; therefore, some attempts such as bio-imprinting [23], immobili~~z~~sation onto different supports [24–27] and optimisation of reaction medium [28] ~~were~~have been made to overcome this drawback. The issue of enzyme instability under repetitive or prolonged use and excess substrate and product inhibitions is common and is usually addressed by immobilisation. Among the several available immobilisation methods, entrapment into beads, i.e. encapsulation, is an advantageous one, because it does not involve any chemical modification of the enzyme. Furthermore, the immobilisation procedure carried out through encapsulation of enzymes in alginate gels is characterised by very mild conditions, easiness of use and low cost.

Based on this background, the purpose of this study was to evaluate the modifications and stability occurring after interaction between tannase and alginate matrix when fabricating alginate beads. To this purpose, we prepared calcium alginate beads either in bare or in tannase-loaded form, and characterised them using several analytical techniques. Preliminary imaging was carried out by both optical and scanning electron microscopy. The presence of tannase in the loaded alginate beads was assessed by chemical analysis via vibrational spectroscopy. The effect of tannase on the bead thermal stability was also investigated by Differential Scanning Calorimetry and Thermogravimetric Analysis, while X-ray diffraction was used to characterise the possible crystalline nature of the bead chemical structure.

~~2.~~2 Experimental

~~2.1.~~2.1 Materials and beads fabrication

All the following analytical grade reagents were purchased from Sigma-Aldrich (Milan, Italy): sodium alginate with number-molecular weight of 12.000–40.000 g/mol, guluronic acid-to-mannuronic acid chains ratio of 40% and dehydrated calcium chloride. Tannase from *Aspergillus ficuum* with 99% purity, 227 U/mL activity (corresponding to 2272 U/mg protein) and molecular weight of 300.000 g/~~mole~~mol was purchased from Shaanxi Sangherb Bio-Tech (Xian, Shaanxi, China).

The sodium alginate powder was sterilized by streaming (134 °C, 4 min) before use. Aqueous solutions of sodium alginate were prepared by dissolving it in ultrapure (milliQ) water (Millipore Super-Q Plus Water Purification System, Bedford, MA, USA) at 3.0% (w/v) concentration stirring for 1 h at 2000 rpm and 25 °C. Under these conditions, a nominal viscosity of 4.0 cP was expected [29]. The alginate solution was then filtered using a membrane filter with 0.2 µm-pore diameter (Millipore, Bedford, MA, USA) and let undisturbed for 30 min to remove air bubbles. Separately, 50 mg of tannase were uniformly dissolved in 5.0 mL of 90 mM citric acid buffer at pH 5.0 and maintained without agitation at room temperature for 30 min. To prepare the alginate composite, the two solutions were then brought together and mixed under the same conditions for 20 min. An apparatus with peristaltic pump was used to vehicle liquids in a terminal syringe. The alginate solution was forced through a polyurethane tube to a 10 mL-glass syringe with 0.3 mm-diameter needle and cast drop-by-drop in a beaker containing a 2.0% (w/v) solution of calcium chloride used as a cross-linker. A typical hypodermic needle was able to produce beads with diameter in the range 0.5–2.0 mm. The resulting beads, having initially grey color, were left to cure in the same calcium chloride solution for 0.5–2.0 h, washed with milliQ water, suspended in a 20 mM sodium phosphate buffer solution, pH 7.3, and stored in a refrigerator at 4 °C, where they were stable for several months before collapsing. The beads picked up for use were washed with distilled water and dried overnight. The cohesive force and shape of tannase-loaded alginate beads may have been mainly due to electrostatic interactions among carboxylic groups of alginate and lateral hydroxyl and amino groups of tannase.

~~2.2.~~2.2 Optical and scanning electron microscopies

Drops of calcium alginate bead suspension were picked up and cast onto a standard optical microscope slide for inspection at low magnification (10× or 20×). Typically, groups of 3–4 agglomerated beads appeared in the samples, which allowed us to check the general bead morphology, i.e. typical size and shape. A calibrated eyepiece with micrometer scale was used for calculation of the bead size, with approximate resolution of 10 µm. At least 100 beads for each formulation were identified and metered to determine the average size.

Scanning electron microscopy (SEM) was also used ~~out~~ to ~~provide~~allow for high resolution inspection of the beads surface. A SEM, model JSM-6360 (JEOL, Akishima~~shi~~, Japan), was used at 15 kV beam energy. After surface dehydration in a desiccator for 2 h, the beads were mounted on aluminium stubs by means of carbon sticky tape supplemented with silver paste, and then coated with 20 nm gold film by sputtering in an argon atmosphere.

~~2.3.~~2.3 Thermogravimetric analysis and differential scanning calorimetry

To remove traces of phosphate buffer, the beads were washed in milliQ water, dried in a vacuum oven at 40 °C for 2 h and stored in a desiccator overnight. Differential scanning calorimetry (DSC) was carried out using a DSC-3 STARe System (Mettler-Toledo, Zurich, Switzerland). Approximately 10 mg of bead samples of ~~each~~either type were loaded in an aluminium pan, while an empty pan was used as the reference. Temperature calibration was performed using indium at the same heating rate. Instrumental temperature accuracy was estimated to be ±0.2 °C. The samples were heated from 25 to 300 °C at a heating rate of 10 °C/min, under constant purging of dry nitrogen at 30 mL/min.

Thermogravimetric analysis (TGA) was carried out by means of a TGA-1/200W STARe System (Mettler-Toledo). Before analysis, optical microscopy inspection was carried out on a bead microtome section and dried in a vacuum oven at 40 °C for 2 h to ascertain the absence of major quantities of absorbed water and gases in the alginate beads. Temperature was ramped from room temperature to 350 °C at a rate of 10 °C/min in nitrogen atmosphere. Differential thermogravimetric (DTG) curves were obtained as the first derivatives of thermograms to stress the mass losses during sample degradation and allow for their easier identification.

~~2.4.~~2.4 Fourier-transform infrared analysis

The Fourier-transform infrared (FTIR) spectra were collected with a spectrometer, model FTIR-8400 (Shimadzu, Kyoto, Japan). All the samples were ground into powders, mixed with potassium bromide and compressed into disks at 600 kg/cm^2 to obtain solid samples. The spectra were collected in the range of 4000–400 cm^{-1} with a resolution of 2 cm^{-1} at 16 scans per spectrum. Fourier self-deconvolution was done with an exponential filter that sharpened the spectral features. To reduce the apparent noise in the data correlated with Fourier self-convolution, a smoothing filter was applied.

~~2.5.~~2.5 X-ray diffractometry

Bead samples were analysed for X-ray diffraction (XRD) in a wide-angle X-ray diffractometer, model D/max-2550 PC (Rigaku, Akishima, Japan). The instrument was equipped with a Rigaku Miniflex goniometer and operated in a continuous mode in increments of 1°/min and scanned over a 2θ range of 10 to 90°. The samples were irradiated with monochromatic Cu Kα radiation (1.542 Å) and analysed between 10 and 60° (2θ). The voltage and current used were 30 kV and 30 mA, respectively. The range and the chart speed were 2 × 10^4 cps and 10 mm/2θ, respectively.

~~3.~~3 Results and discussion

~~3.1.~~3.1 Beads morphology

Before carrying out the thermal stability (DSC, TGA), chemical composition (FTIR) and structural (XRD) analyses, we have first examined the beads morphology either at low magnification by light microscopy or at high magnification by SEM. Examples of optical micrographs of the beads illustrated in Fig. 1 show that the structure morphology (panel a) was maintained after tannase entrapment (panel b), with no significant difference in size. Under the conditions used here, both bare and tannase-loaded alginate beads showed almost the same size, with equivalent diameter in the range of 1.4–1.9 mm and an average value of about 1.6 mm, as well as oval shape due to a significant content of water in buffer phosphate, pH 7.3 (panels a and b). After drying without special precautions directly in the SEM chamber, the beads morphology was strongly altered, with major shrinkage of the respective volumes (panels c and d) and an apparently different behaviour. These differences were evident also in the high magnification views of the respective surfaces (panels e and f). The stability of tannase-loaded alginate beads (panel d) may have been the result of a lower number of hydrophilic groups compared with bare alginate; therefore, exposition to drying may have exerted lesser effects due to a reduction of hydration molecules on the bead surface.

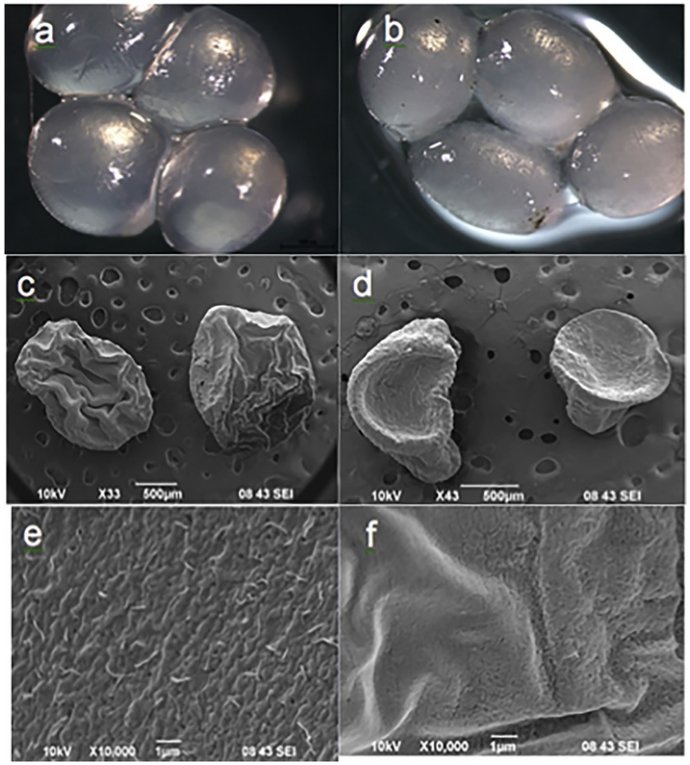

~~**Figure 1:**~~**Fig. 1** Images of bare (a, c, e) and tannase-loaded (b, d, f) alginate beads, under optical microscope (a, b, 20~~x~~x) and SEM (c – f). High resolution images showing the different surface morphology of e) bare and f) tannase-loaded beads.

alt-text: Fig. 1

The bead surface after drying appeared to become rough and exhibited many wrinkles. Small burs were visible on the surface, and cracks of the gold coating appeared occasionally on the surface of both bead types (results not shown), due to the volume shrinkage after drying. However, the microscale roughness appeared different in nature. In bare alginate beads (Fig. 1, panel e) fibres appeared on the surface, whereas in the tannase-loaded ones (Fig.1, panel f) these features were absent and the surface grains smaller, providing an overall more compact surface. The uniformity of these surfaces is also a hint that tannase was dispersed uniformly in the polymer matrix.

~~3.2.~~3.2 Thermal analysis

Differential scanning calorimetry (DSC) was used to characterise the thermal behaviour of beads. DSC thermograms of both types of beads are illustrated in Fig. 2~~, panels a and b~~. Lower temperature endothermic peaks, observed in heating curves of both types of beads, most probably denote desorption of physically a~~b~~dsorbed water and removal of structural water [30]. However, the bare alginate beads exhibited an endothermic peak with about twice the intensity of that of the beads with entrapped tannase at lower temperature (108 °C vs 116~~o~~ °C), although the enthalpy values of the overall process were rather similar (2028 J/g vs 2078 J/g). Degradation of both types of beads probably started above 200~~o~~ °C (panel b), as the likely result of dehydration of saccharide rings, as well as breaking up of C-H bonds and C-O-C glycoside bonds in the main polysaccharide chain [31].

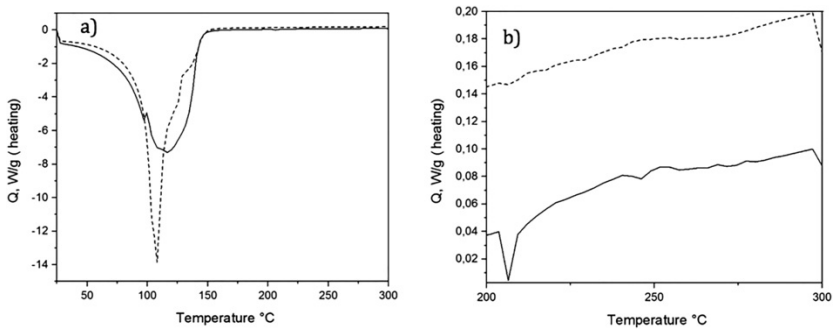

~~Figure 2.~~Fig. 2 DSC curves (a - total heating thermogram, b - excerpt from the total heating thermogram in the temperature range 200–300 °C) of alginate beads (dashed line) and tannase-loaded beads (continuous line), recorded in nitrogen atmosphere.

alt-text: Fig. 2

According to DSC data, TGA profiles can be analysed within two steps: a former step occurring in the range 25–175 °C and a latter occurring in the range 175–300 °C (Fig. 3a–b).

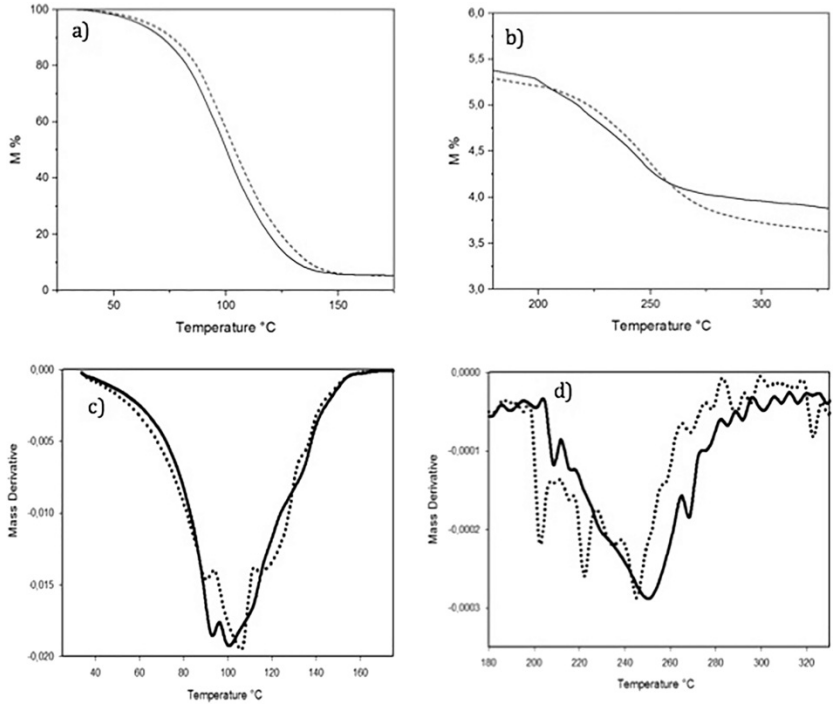

~~Figure 3.~~Fig. 3 TGA (a, b) and 1st derivative (c, d) curves of alginate beads (dashed line) and tannase-loaded beads (continuous line), recorded in nitrogen atmosphere.

alt-text: Fig. 3

As discussed above, the former step, accounting for about 94% of weight loss, can be attributed to the desorption of physically ~~a~~bsorbed water and removal of structural water, hence denoting excellent water absorption characteristics of both types of beads, while the latter to the decomposition of polymer part of alginate beads. However, thermal decomposition behaviour of both alginate and alginate/tannase beads was rather similar, only minor differences being visible in the DTG curves (Fig. 3c–d).

~~3.3.~~3.3 Fourier-transform infrared analysis

The FTIR spectrum of bare calcium alginate beads is shown in Fig. 4, panel a. In the high frequency region, the stretching vibrations of O—H bonds of alginate appear in the wavenumber range from 3000 to 3600 cm^{-1} [32], while stretching vibrations of aliphatic C—H are observed at 2920–2850 cm^{-1}. The bands around 1649 cm^{-1} can be attributed to the carboxylate ion, the one at 1460 cm^{-1} to the asymmetric and symmetric stretching vibrations, and those at 1107 and 935 cm^{-1} to the C—O stretching vibration of ring and the C—O stretching with contributions from C—C—H and C—O—H deformation. The stretching of the C=O group of the undissociated carboxylic group is also detected at 1730 and 1631 cm^{-1}, as reported for alginate films [33]. Additionally, bands appearing around 800 and 700 cm^{-1} can be assigned to mannuronic and guluronic acids, respectively [34,35], which are both present in the alginate structure.

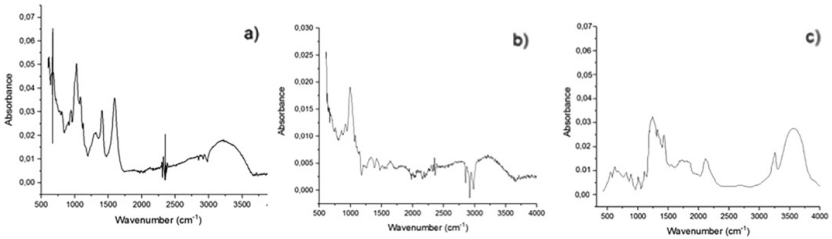

~~Figure 4:~~Fig. 4 FTIR spectra of a) calcium alginate beads, b) pure tannase, and c) tannase-loaded calcium alginate beads.

alt-text: Fig. 4

It is noteworthy that the asymmetric stretching vibration of the carboxylate ion (1620–1598 cm^{-1}) is shifted to lower wavenumbers in comparison with that expected for sodium alginate [36]. Such a shift may have been due not only to the interaction of the regular homopolymeric chain with sodium ions, but also to the change in cation density, radius and atomic weight when Ca^{2+} replaced Na^{+}. One can see that the absorption region of O—H stretching vibrations of calcium alginate beads is narrower than that of sodium alginate [36]. Such a difference was likely due to the interaction of alginate hydroxyl and carboxylate groups with Ca^{2+} when forming the chelating structure, and to the consequent decrease in the number of hydrogen bonds among OH groups.

The FTIR spectrum of the free tannase showed vibration frequency bands at 3432, 2838, 2086, 1632, 1367 and 781 cm^{-1}, hence reflecting the presence of O—H stretching, C—H stretching, conjugated C—O, aromatic C—C, C—O stretching and para O—H (out of plane) (Fig. 4, panel b).

As far as the FTIR spectrum of the tannase-loaded beads is concerned (Fig. 4, panel c), the fingerprint region (650–1300 cm^{-1}) appears to be much richer in characteristic peaks than that of the bare beads. This region includes the contributions from complex interacting vibrations, giving rise to the generally unique fingerprint of each compound. Additionally, the peaks shift in wavenumber and decrease in intensity clearly demonstrate that there were

interactions among alginate, tannase and Ca^{2+}. Probably, the tannase hydroxyl groups were able to form intermolecular hydrogen bonds with alginate and shared with it the Ca^{2+} coordination site. Similar Ca^{2+} coordination may be ascribed to the carboxyl groups of tannase.

~~3.4.~~3.4 X-ray diffraction

To investigate the entrapment of tannase in the calcium alginate beads as well as its possible effect on the physical state of the alginate matrix, X-ray diffraction (XRD) data have been acquired.

The curve “a” in Fig. 5 shows the XRD pattern of bare calcium alginate beads. One can see two major crystalline peaks at 2θ diffraction angles of 13 and 22°. Observation of comparable micro-crystallites has already been reported in amorphous structure [37,38], and characteristic peaks for calcium alginate are known to appear at angles of 13°, 56°, 20.64°, 20.06°, 28.96° and 36~~,~~-40°, thus demonstrating its semi-crystalline nature [39,40]. Actually, alginate is a linear polysaccharide composed of poly-β-1,~~-~~4-D-mannuronic acid (M) and ~~β~~α-1,~~-~~4-L-guluronic acid (G) residues in various ratios, which are arranged in MM or GG blocks interspersed with MG blocks [41]. Such semi-crystallinity disappear~~s~~ed in the tannase-loaded beads corresponding to the line “b” of Fig. 5. This observation clearly indicates that the enzyme was present in an amorphous state in the matrix, inducing a change in its crystalline state. One of the reasons for this is that the gelation process changed the spatial structure of alginate, or even that an intermolecular interaction occurred between tannase and alginate. Similar transition from a crystalline form to an amorphous one has already been observed in alginate beads [42,43]. Since tannase has a molecular weight of 300 kDa, this feature offers an advantage in terms of mixing between compounds. Moreover, it is a hetero-octamer with two subunits able to interfere with the alginate semi-crystallinity order during the beads preparation. The presence of the internal strain might be the reason for fracturing the grains into sub-grains, which may have led to a decrease in crystallite size of tannase-loaded beads.

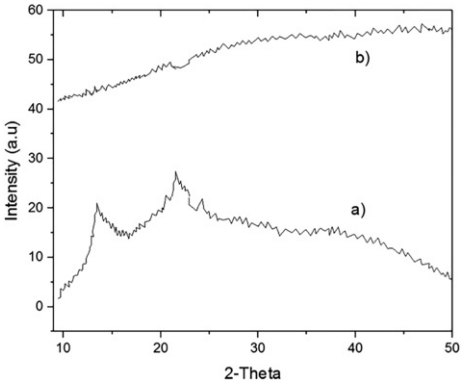

~~Figure 5.~~Fig. 5 XRD pattern of calcium alginate beads (line a) and tannase-loaded calcium alginate beads (line b).

alt-text: Fig. 5

~~4.~~4 Conclusions

In this work, tannase-loaded calcium alginate beads were successfully prepared by gelation and stabilized in phosphate buffer at pH 7.3. The preparation method is simple, fast, consistent, inexpensive, and can be carried out under mild conditions in an aqueous environment at room temperature. Detailed characterisation has been carried out by SEM, DSC, TGA, FTIR and XRD techniques. In particular, SEM micrographs revealed remarkable changes in the bead surface structure, and FTIR showed the corresponding change in the bead contents, confirming the entrapment of tannase. XRD analysis demonstrated that tannase entrapment induced a structural grain change in the alginate gel from a crystalline state to an amorphous one. The results of this study suggest that the prepared polymer system could be used in food applications in the near future, for example to improve tea quality or clarify juices, or for controlled release of the enzyme. Finally, the results obtained may be considered of general interest for possible formulation of tannase in polysaccharide composites.

Acknowledgements

This work was supported by CAPES (Coordenação de Aperfeiçoamento de Pessoal de Nível Superior, grant number 88881.131854/2016-01)~~,~~ ~~CNPq (Conselho Nacional de Desenvolvimento Científico e Tecnológico) and FACEPE (Fundação de Amparo a Ciência e Tecnologia de Pernambuco)~~. Moreover, the authors would like to acknowledge the networking support by the COST Action CA15107 Multi-Functional Nano-Carbon Composite Materials Network (Multi Comp), and Claudio Larosa acknowledges the support of CA15107 Short Term Scientific Missions (STSMs, grant number 40735).

Competing interests

All authors declare that they have agreed to publish this paper and that there are no competing interests.

References

[1] M.G. Dekamin, Z. Karimi, Z. Latifidoost, S. Ilkhanizadeh, H. Daemi, M.R. Naimi-Jamal and M. Barikani, Alginic acid: a mild and renewable bifunctional heterogeneous biopolymeric organocatalyst for efficient and facile synthesis of polyhydroquinolines, *Int. J. Biol. Macromol.* **108**, 2018, 1273–1280.

[2] S. Opasanon, P. Muangman and N. Namviriyachote, Clinical effectiveness of alginate silver dressing in outpatient management of partial-thickness burns, ~~*Int. Wound. J.*~~*Int. Wound J.* **7**, 2010, 467–471.

[3] M. Rajaonarivony, C. Vauthier, G. Couarraze, F. Puisieux and P. Couvreur, Development of a new drug carrier made from alginate, *J. Pharm. Sci.* **82**, 2018, 912–917.

[4] P. Sriamornsak and S. Sungthongjeen, Modification of theophylline release with alginate gel formed in hard capsules, *AAPS PharmaSciTech.* **8**, 2007, E1–E8.

[5] J. Li, S.Y. Kim, X. Chen and H.J. Park, Calcium-alginate beads loaded with gallic acid: preparation and characterization, *LWT - Food Sci Technol.* **68**, 2016, 667–673.

[6] E. Hermansson, E. Schuster, L. Lindgren, A. Altskär and A. Ström, Impact of solvent quality on the network strength and structure of alginate gels, ~~*Carbohydr Polym.*~~*Carbohydr. Polym.* **144**, 2016, 289–296.

[7] H.H. Tønnesen and J. Karlsen, Alginate in drug delivery systems, *Drug Dev. Ind. Pharm.* **28**, 2002, 621–630.

[8] R.D. Cheshmeh, G.S. Khorramabadi, A.R. Khataee and S. Jorf, Silica nanopowders/alginate composite for adsorption of lead (II) ions in aqueous solutions, *J. Taiwan Inst. Chem. Eng.* **45**, 2014, 973–980.

[9] A.Z.M. Badruddoza, A.S.H. Tay, P.Y. Tan, K. Hidajat and ~~M.S~~M.S. Uddin, Carboxymethyl-β-cyclodextrin conjugated magnetic nanoparticles as nano-adsorbents for removal of copper ions: synthesis and adsorption studies, *J. Hazard Mater.* **185**, 2011, 1177–1186.

[10] F. Googerdchian, A. Moheb and R. Emadi, Lead sorption properties of nanohydroxyapatite – alginate composite adsorbents, *Chem. Eng. J.* **200–202**, 2012, 471–479.

[11] P.K. Lekha and B.K. Lonsane, Production and application of tannin acyl hydrolase: state of the art, *Adv. Appl. Microbiol.* **44**, 1997, 215–260.

[12] S.S.N. Maharachchikumbura, *Pestalotiopsis* — morphology, phylogeny, biochemistry and diversity, *Fungal Divers.* **50**, 2011, 167–187.

[13] S. Mandal, S.S. Kumar, B. Krishnamoorthy and S.K. Basu, Development and evaluation of calcium alginate beads prepared by sequential and simultaneous methods, *Braz. J. Pharm. Sci.* **46**, 2010, 785–793.

[14] E. Chan, B. Lee, P. Ravindra and D. Poncelet, Prediction models for shape and size of Ca-alginate macrobeads produced through extrusion – dripping method, ~~*J. Colloid. Interface Sci.*~~*J. Colloid Interface Sci.* **338**, 2009, 63–72

[15] R. Belmares and J.C. Contreras-Esquivel, Microbial production of tannase: an enzyme with potential use in food industry, *LWT-Food Sci. Technol.* **37**, 2004, 857–864.

[16] S. Sharma and M.N. Gupta, Synthesis of antioxidant propyl gallate using tannase from *Aspergillus niger* van Teighem in nonaqueous media, *Bioorg. Med. Chem. Lett.* 2002, 395–397.

[17] X. Yu, Y. Li and D. Wu, Microencapsulation of tannase by chitosan – alginate complex coacervate membrane: synthesis of antioxidant propyl gallate in biphasic media, *J. Chem. Technol. Biotechnol.* **479**, 2004, 475–479

[18] A.B. El-Tanash, A.A. Sherief and A. Nour, Catalytic properties of immobilized tannase produced from *Aspergillus aculeatus* compared with the free enzyme, *Braz. J. Chem. Eng.* **28**, 2011, 381–391.

[19] S. Kumar, V. Beniwal, N. Kumar, A. Kumar, V. Chhokar and T.P. Khaket, Biochemical characterization of immobilized tannase from *Aspergillus awamori*, *Biocatal. Agric. Biotechnol.* **4**, 2015, 398–403.

[20] M.-J. Lu and C. Chen, Enzymatic modification by tannase increases the antioxidant activity of green tea, *Food Res. Int.* **41**, 2008, 130–137.

[21] M.-J. Lu, S.-C. Chu, L. Yan and C. Chen, Effect of tannase treatment on protein-tannin aggregation and sensory attributes of green tea infusion, *LWT – Food Sci. Technol.* **42**, 2009, 338–342.

[22] B.G. Mendes, M.J. Machado and M. Falkenberg, Screening of glycolipids in medicinal plants, *Rev. Bras. Farmacogn.* **16**, 2006, 568–575.

[23] W. Liu, B. Zhang, Q. Wang, Z. Xie, W. Yao, X. Gao and L.L. Yu, Effects of sulfation on the physicochemical and functional properties of *Psyllium*, ~~*J. Agric. Food. Chem.*~~*J. Agric. Food Chem.* **58**, 2010, 172–179.

[24] A. Srivastava and R. Kar, Application of immobilized tannase from *Aspergillus niger* for the removal of tannin from myrobalan juice, *Indian J. Microbiol.* **50**, 2010, 46–51.

[25] C.N. Aguilar, R. Rodríguez and J.C. Contreras-Esquivel, Microbial tannases: advances and perspectives, *Appl. Microbiol. Biotechnol.* **76**, 2007, 47–59.

[26] J.S. Lima, M.P. Cabrera, C.M.S. Motta, A. Converti and L.B. Carvalho, Jr., Hydrolysis of tannins by tannase immobilized magnetic diatomaceous earth nanoparticles coated with polyaniline, *Food Res. Int.* **107**, 2018, 470–476.

[27] R. Li, F.G. Fu, C. Liu, Y. Wan, S. Wang and T. Liu, Tannase immobilisation by amino-functionalised magnetic Fe3O4-chitosan nanoparticles and its application in tea infusion, *Int. J. Biol. Macromol.* 2018, https://doi.org/10.1016/j.ijbiomac.2018.03.077.

[28] X. Yu, Y. Li, S. Zhou and Y. Zheng, Synthesis of propyl gallate by mycelium-bound tannase from *Aspergillus niger* in organic solvent, *World J. Microbiol. Biotechnol.* **23**, 2007, 1091–1098.

[29] S. Fu, A. Thacker, D.M. Sperger, R.L. Boni, S. Velankar, E.J. Munson and L.H. Block, Rheological evaluation of inter-grade and inter-batch variability of sodium alginate, *AAPS PharmSciTech* **11**, 2010, 1662–1674.

[30] M. Etcheverry, V. Cappa, J. Trelles and G. Zanini, Montmorillonite-alginate beads: natural mineral and biopolymers based sorbent of paraquat herbicides, *J. Environ. Chem. Eng.* **5**, 2017, 5868–5875.

[31] D. Plackett, Biopolymers: New Materials for Sustainable Films and Coatings, 2011, John Wiley & Sons; New York.

[32] A. Manuja, S. Kumar, N. Dilbaghi, G. Hanjana, M. Chopra, H. Kaur, R. Kumar, B.K. Manuja, S.K. Singh and S.C. Yadav, Quinapyramine sulfate-loaded sodium alginate nanoparticles show enhanced trypanocidal activity, *Nanomedicine* **9**, 2014, 1625–1634.

[33] C.K. Yeom and K. Lee, Characterization of sodium alginate membrane crosslinked with glutaraldehyde in pervaporation separation, *J. Appl. Polym. Sci.* **67**, 1997, 209–219.

[34] G. Cardenas-Jiron, D. Leal and B. Matsuhiro, Vibrational spectroscopy and density functional theory calculations of poly-D-mannuronate and heteropolymeric fractions from sodium alginate, *J. Raman Spectrosc.* **42**, 2011, 870–878.

[35] N.P. Chandia, B. Matsuhiro and A.E. Vasquez, Alginic acids in *Lessonia trabeculata*: characterization by formic acid hydrolysis and FT-IR spectroscopy, *Carbohydrate Polym.* **46**, 2001, 81–87.

[36] H. Daemi and M. Barikani, Synthesis and characterization of calcium alginate nanoparticles, sodium homopolymannuronate salt and its calcium nanoparticles, *Sci. Iran.* **19**, 2012, 2023–2028.

[37] R.W. Collins, A.S. Ferlauto, G.M. Ferreira, C. Chen, J. Koh, R.J. Koval, Y. Lee, J.M. Pearce and ~~C.R~~C.R. Wronski, Evolution of microstructure and phase in amorphous, protocrystalline, and microcrystalline silicon studied by real time spectroscopic ellipsometry, *Sol. Energy Mater. Sol. Cells* **78**, 2003, 143–180.

[38] S.R. Herd and P. Craudhari, On the question of microcrystallites in some amorphous materials. An electron microscope investigation, *Phys. Status Solidi A-Appl. Mat.* **26**, 1974, 627–642.

[39] M. Rudee and ~~A~~A. Owie, The structure of amorphous Si and Ge, *Philos. Mag.* **25**, 1972, 1001–1007.

[40] K.V. Sri, A. Kondaiah, J.V. Ratna and A. Annapurna, Preparation and characterization of quercetin and rutin cyclodextrin inclusion complexes, *Drug Dev. Ind. Pharm.* **33**, 2007, 245–253.

[41] S. Holtan, P. Bruheim and G. Skjåk-Bræk, Mode of action and subsite studies of the guluronan block-forming mannuronan C-5 epimerases AlgE1 and AlgE6, *Biochem. J.* **395**, 2006, 319–329.

[42] J. Xing, D. Zhang and T. Tan, Studies on the oridonin-loaded poly (D,L-lactic acid) nanoparticles in vitro and in vivo, *Int. J. Biol. Macromol.* **40**, 2007, 153–158.

[43] T.H. Wu, F.L. Yen, L.T. Lin, T.R. Tsai, C.C. Lin and ~~T.M~~T.M. Cham, Preparation, physicochemical characterization, and antioxidant effects of quercetin nanoparticles, *Int. J. Pharm.* **346**, 2008, 160–168.

Highlights

- *Aspergillus ficuum* tannase is successfully entrapped in calcium alginate beads.
- Tannase-containing beads are physically characteri~~z~~sed by XRD, FTIR and DSC/TGA.

- Non-crystalline tannase-loaded beads are suitable as carrier for controlled release.
- Tannase-loaded beads may also be used to clarify juices and to improve tea quality.

Queries and Answers

Query:

Your article is registered as a regular item and is being processed for inclusion in a regular issue of the journal. If this is NOT correct and your article belongs to a Special Issue/Collection please contact p.dubay@elsevier.com immediately prior to returning your corrections.

Answer: Yes

Query:

Please confirm that given names and surnames have been identified correctly and are presented in the desired order, and please carefully verify the spelling of all authors' names.

Answer: Yes

Query:

The author names have been tagged as given names and surnames (surnames are highlighted in teal color). Please confirm if they have been identified correctly.

Answer: In the case of the fourth author, Merijs Meri should be considered as Surname.

Query:

Please provide the corresponding grant number(s) for the following grant sponsor(s): "CAPES"; "CNPq"; and "FACEPE".

Answer: The CAPES grant number is 88881.131854/2016-01. On the other hand, CNPq and FACEPE can be removed.